





# Quark-Hadron Duality in Neutrino Nucleon Scattering and Analogies in Nuclei

E. A. Paschos  
TU Dortmund , Germany

Oct. 12, 2018 :NuSTEC  
Gran Sasso Institute

- 
- In 1968 the SLAC-MIT experimental group presented their data on DIS for moderate values of  $Q^2$  where the resonances were very evident. At the same time Bjorken proposed the scaling of the data. The experimental results created a debate about whether scaling was really observed. There were many resonances located outside the average curve and some are shown in the next few slides.
  - There were several proposals on how the resonances will merge together and follow a scaling curve. One was based on vector meson dominance; another, the parton model, introduced the scattering of the virtual photon on elementary constituents whose kinematics produced scaling. The question emerged how the resonances are related the scaling in these models.

- 
- The next slides show the data taken for the scattering of electrons at an angle of  $6^\circ$  and at two different initial energies :
    - $\alpha$ ) 7.0 GeV (lower curve) and
    - $\beta$ ) 16.0 GeV (upper curve). At the higher energy the resonances are less prominent.

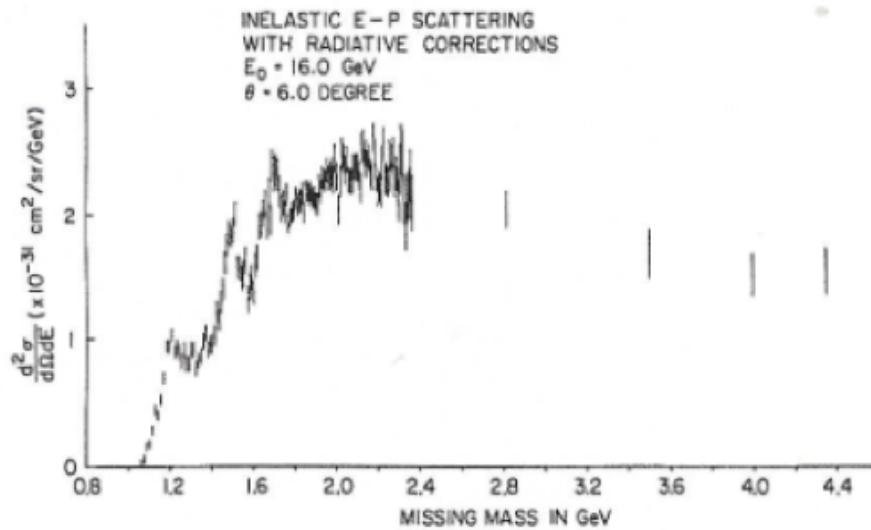


Fig. 14 Figure 13, after radiative correction.

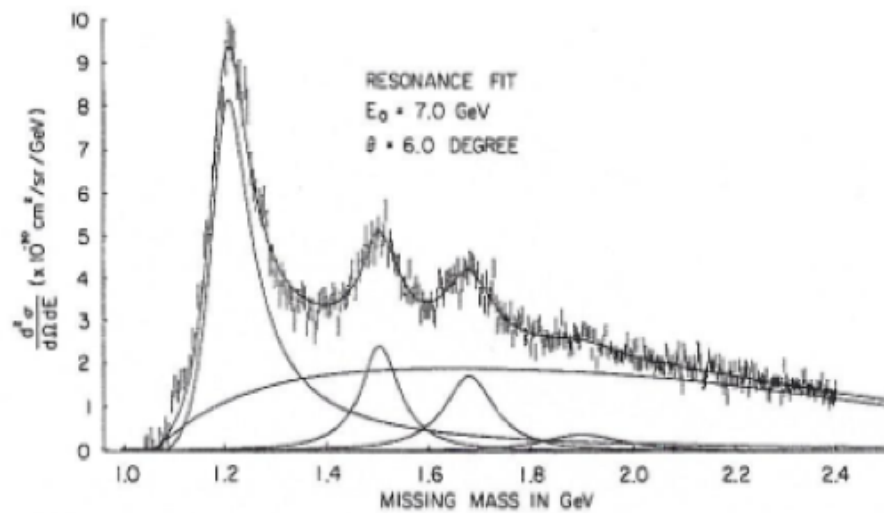
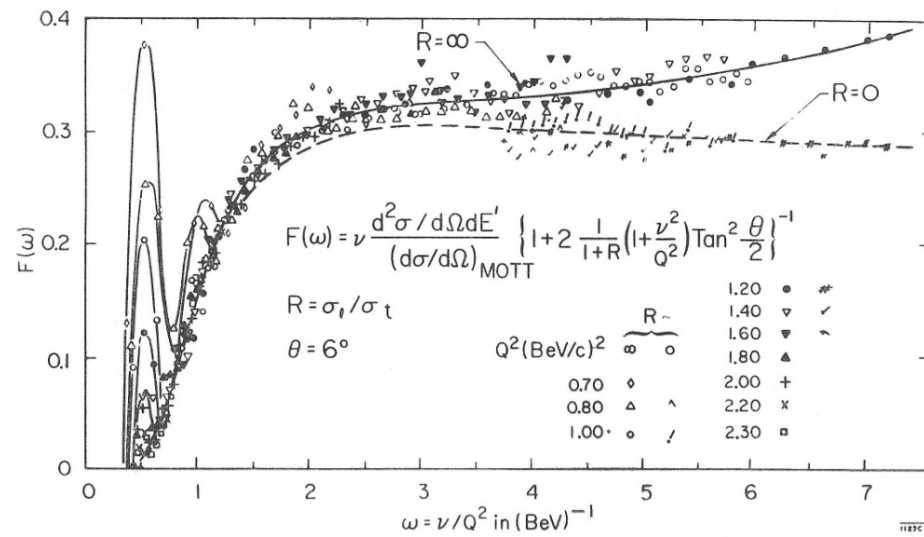



Fig. 15 The inelastic spectrum at 7 GeV,  $6^\circ$ , resolved into Breit-Wigner peaks by a fitting procedure.


The figure from the first publication shows the scaling function  $\nu W_2$  as a function of  $\omega$ . Few resonances are still present.



ΠΡΑΚΤΙΚΑ ΤΗΣ ΑΚΑΔΗΜΙΑΣ ΑΘΗΝΩΝ



- 
- Studying this curve in detail we were motivated to identify the partons with quarks (Bjorken and Paschos, 1969). At soft scattering resonances are formed, but when the interactions become violent, at larger values of  $Q^2$ , the role of the resonances diminishes and the quark content becomes evident. In addition, as the scattered quarks fly out of the proton they recombine with other quarks and convert again to hadrons (final state interactions).

- 
- The disappearance of the resonances is a dynamic effect and may be related to the emergence of the continuum. Bloom and Gilman suggested (1970) that the resonances plotted in the variable

$$\omega' = 1 + W^2/Q^2$$

will slide down the scaling curve as  $Q^2$  increases and they eventually will disappear. This happens when diffraction is absent or subtracted in the process.

---

SCALING, DUALITY, AND THE BEHAVIOR OF RESONANCES  
IN INELASTIC ELECTRON-PROTON SCATTERING\*

E. D. Bloom and F. J. Gilman

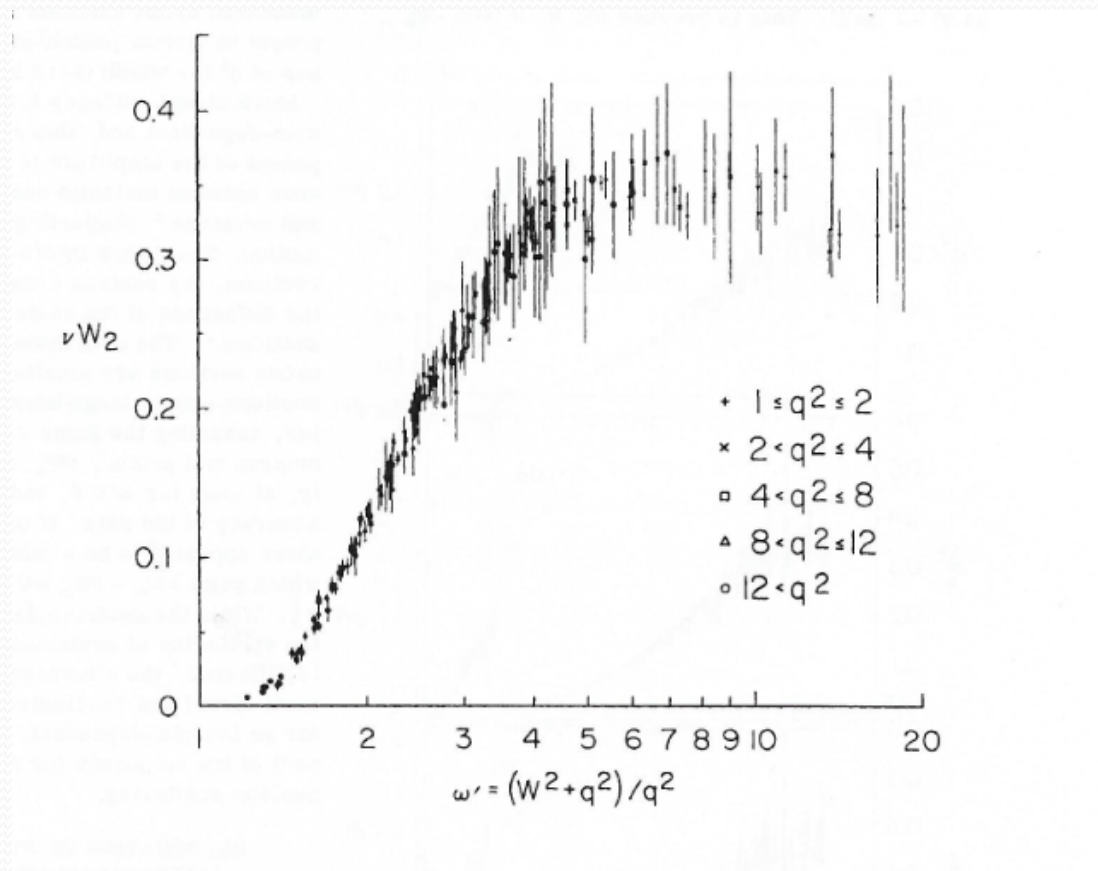
*Stanford Linear Accelerator Center, Stanford University, Stanford, California 94305*

(Received 25 June 1970)

1. The resonances are an intrinsic part of the scaling phenomenon for  $\nu W_2$ .
2. Finite energy sum rules emerge when we integrate over the scaling curves or over the resonances.
3. At that time, the community was still not convinced about quark substructure in protons. In fact in the first article there is no mention of quarks or partons! They compared resonances with hadronic scaling.
4. Variable  $\omega' = 1 + W^2/Q^2 = \omega + M^2/Q^2$



Second article in Phys.Rev. has a cut for  $W > 1.4$  GeV in order to eliminate the dominant resonances and mentions quarks. Scaling is now evident.



More variables were proposed. A new variable is obtained by keeping the mass of the target and setting  $P_x^2=0.0$

$$(q+xp)^2 = p_x^2 \quad \text{for } p^2 = p_x^2 = 0$$

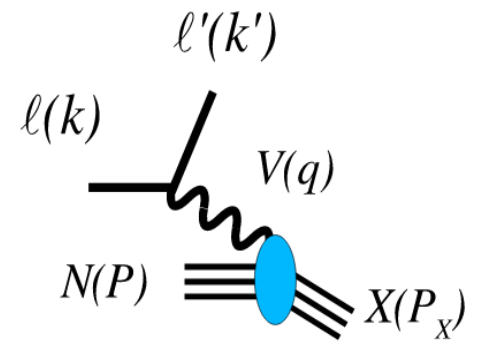
$$x = Q^2/(2Mv) \quad \text{Bjorken}$$

$$\text{For } p^2 = M^2, \quad p_x^2 = 0, \quad (q+\xi p)^2 = -Q^2 + 2Mv\xi + \xi^2 M^2 = 0$$

$$\text{obtain } \xi - x + (M^2 x/Q^2) \xi^2 = 0$$

$$\xi = \frac{2x}{1 + \sqrt{1 + 4x^2 M^2/Q^2}} .$$

Nachtman  
variable



To make the statement quantitative it was suggested that the area over the resonances is on the average the area under the scaling curve. However, the limits of integration were arbitrary.

$$I_i(Q^2) = \frac{\int_{\xi_{\min}}^{\xi_{\max}} d\xi \mathcal{F}_i^{(\text{res})}(\xi, Q^2)}{\int_{\xi_{\min}}^{\xi_{\max}} d\xi \mathcal{F}_i^{(\text{LT})}(\xi, Q^2)}$$

The Adler sum rule for neutrinos demonstrates that we can use the resonances or integrate over the scaling curve.

$$\left[ g_{1V}^{(QE)}(Q^2) \right]^2 + \left[ g_{1A}^{(QE)}(Q^2) \right]^2 + \left[ g_{2V}^{(QE)}(Q^2) \right]^2 \frac{Q^2}{4M^2} + \int d\nu [W_2^{\nu n}(Q^2, \nu) - W_2^{\nu p}(Q^2, \nu)] = 2$$

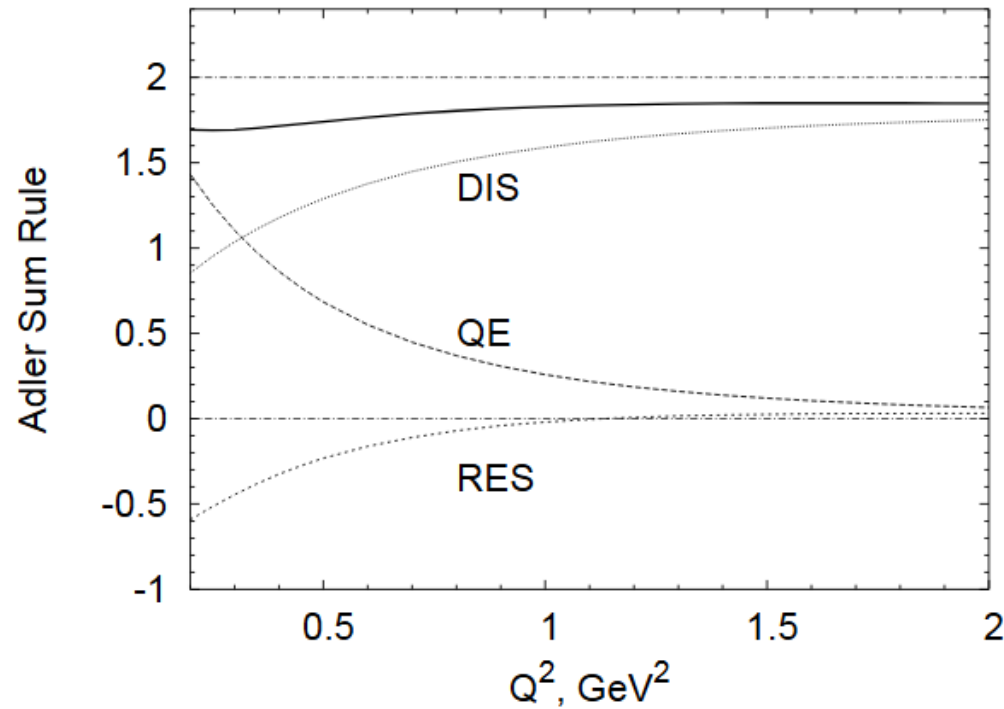
$$\xi_{\min} = \xi(Q^2, W = 1.6 \text{ GeV}) \text{ to } \xi_{\max} = \xi(Q^2, W = 1.1 \text{ GeV}).$$

Sum rule is valid for each value of  $Q^2$ . At low energy we can use either resonances or scaling function for

$$\xi_{\min} < \xi < \xi_{\max}.$$

Beyond the low energy we integrate over structure functions given in leading twist by the MRST parametrization. Diffraction drops out in the difference of structure functions.

Observation: particle sum rules are independent of  $Q^2$ . Thus for the low  $\nu$  region use the resonances and for the remaining region integrate over the scaling curve.



6: Decomposition of the Adler sum, as a function of  $Q^2$ , into its QE (dashed) RES (short dashed) and deep inelastic (dotted) contributions, as well as the total



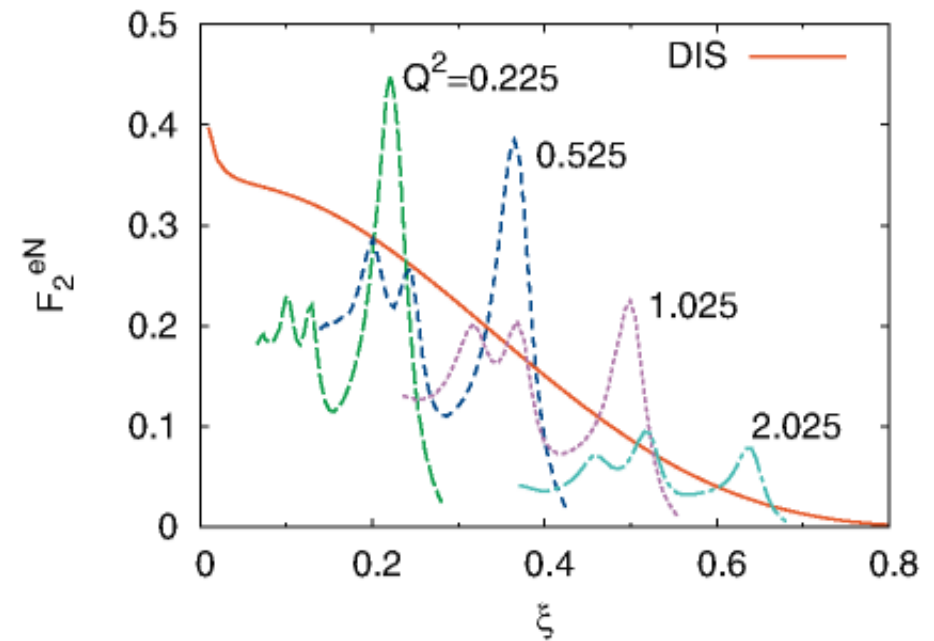
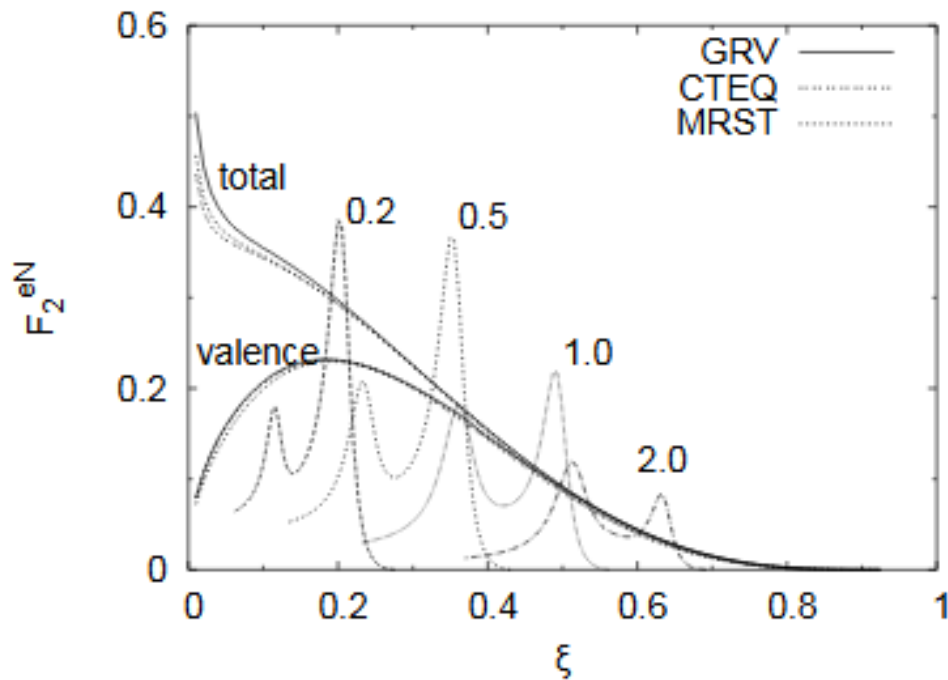
- 
- The previous slide verifies that for

$$Q^2 < 1.0 \text{ GeV}^2$$

the  $\nu$  integration over the resonances is to within 20% equal to the integral over the scaling curve.

Comparisons were carried out for neutrino reactions and were verified for structure functions  $F_2(x)$  and  $F_3(x)$ .

# Structure Function for electroproduction with 4 resonances(left) and 13 resonances(right).



# Difference (resonances – scaling curve) Niculescu and the Jefferson group.

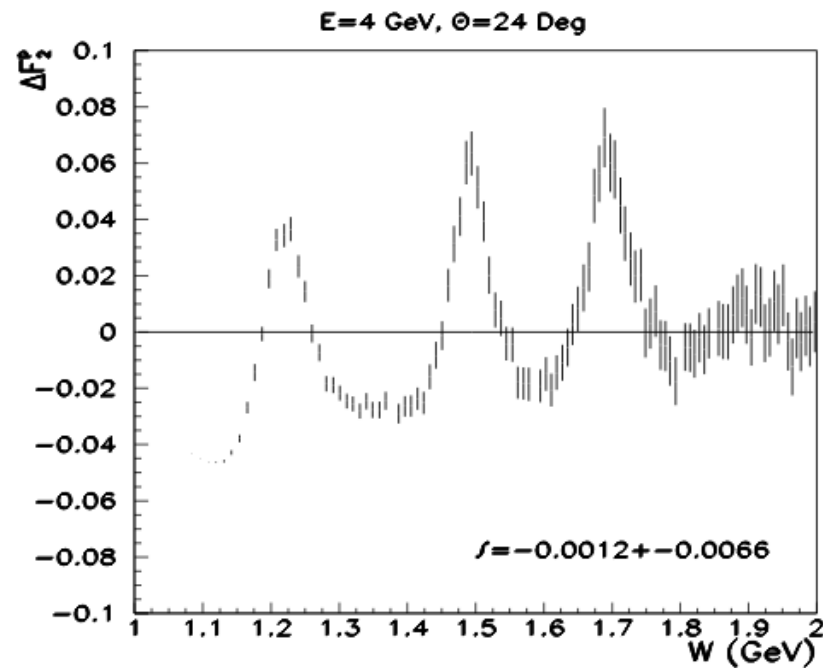
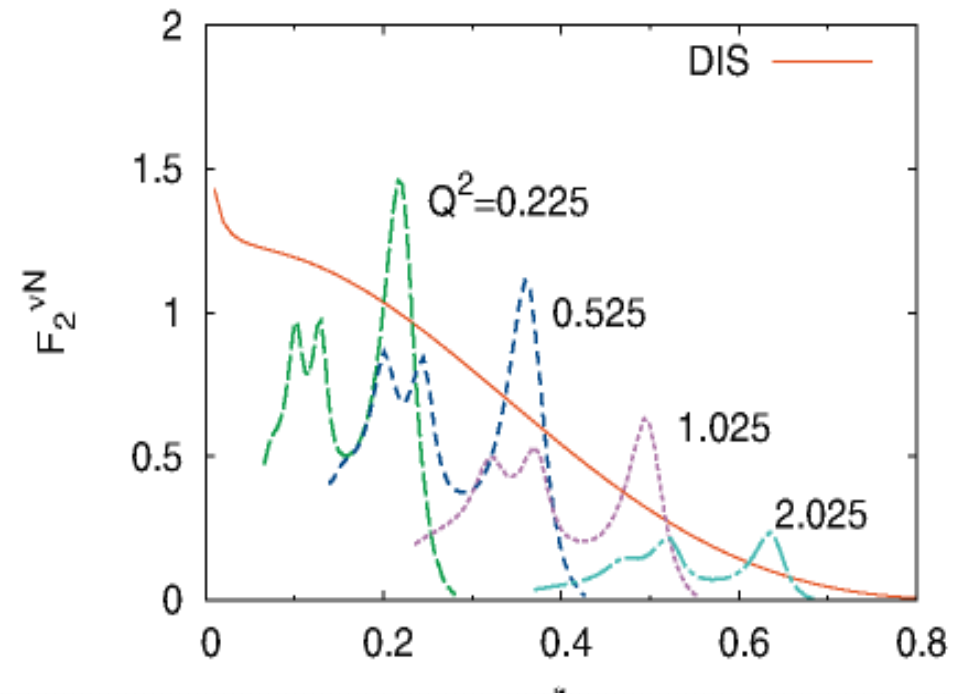
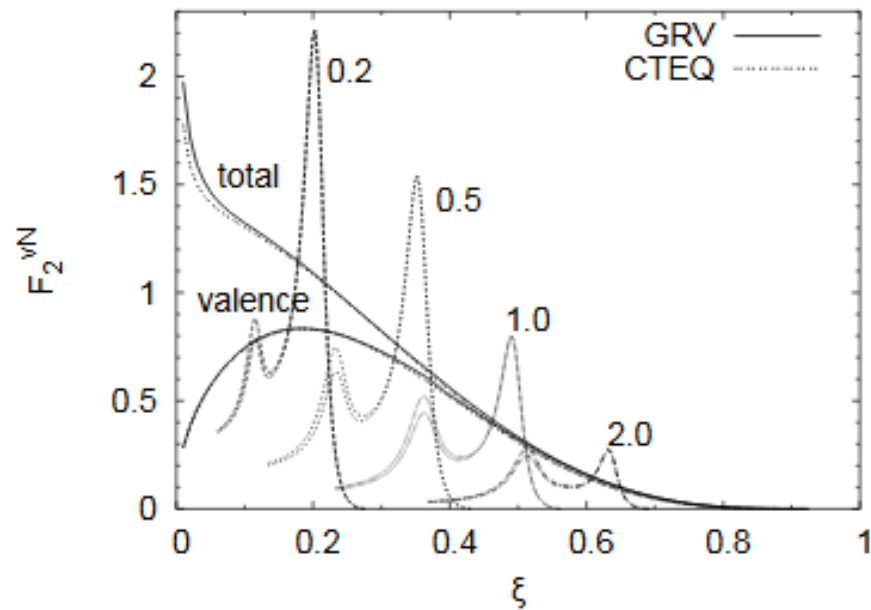


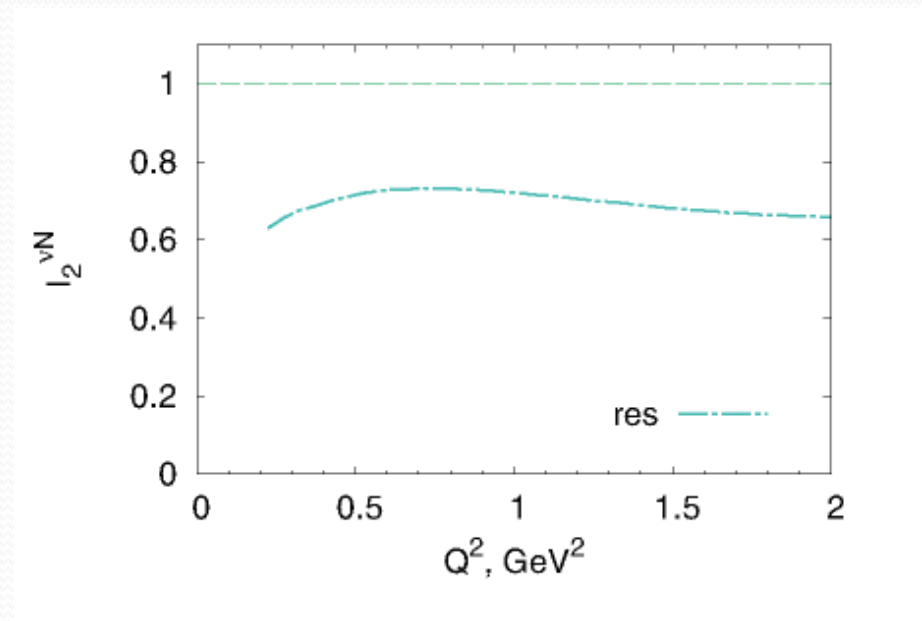
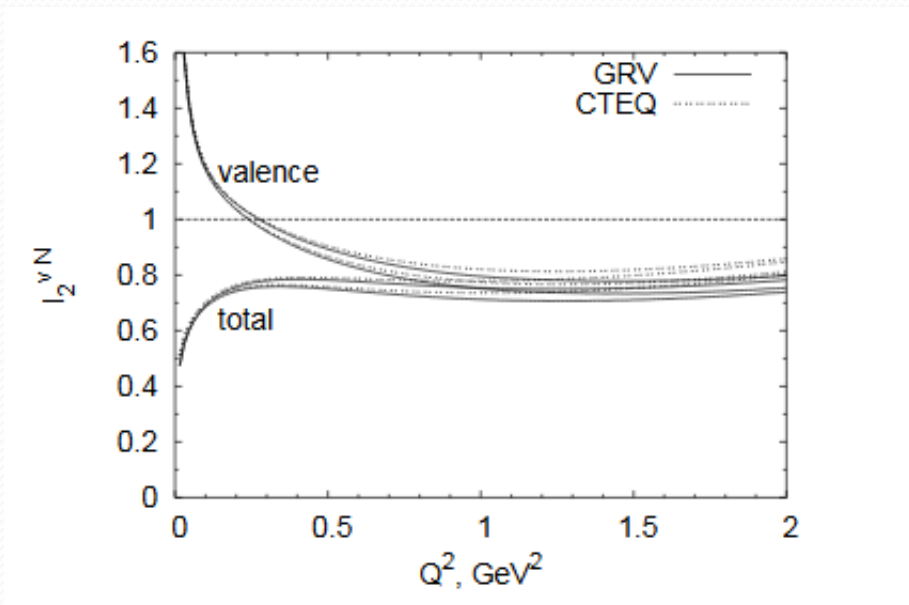
FIG. 15. The difference  $\Delta F_2^p$  between proton  $F_2^p$  structure function data (at the indicated kinematics) from Jefferson Lab Hall C and the scaling curve of Ref. [70] as a function of missing mass  $W$ . The integrated difference yields a value of  $-0.0012 \pm 0.0066$  for this particular  $W$ -spectrum.

# Neutrino on isoscalar target $F_2(\xi)$ vs $\xi$ .

Left Dortmund model; right Giessen (Lalakulich et al.). Except for strange quark contribution, electron and neutrino cross sections on isoscalar are related by a factor of 5/18.



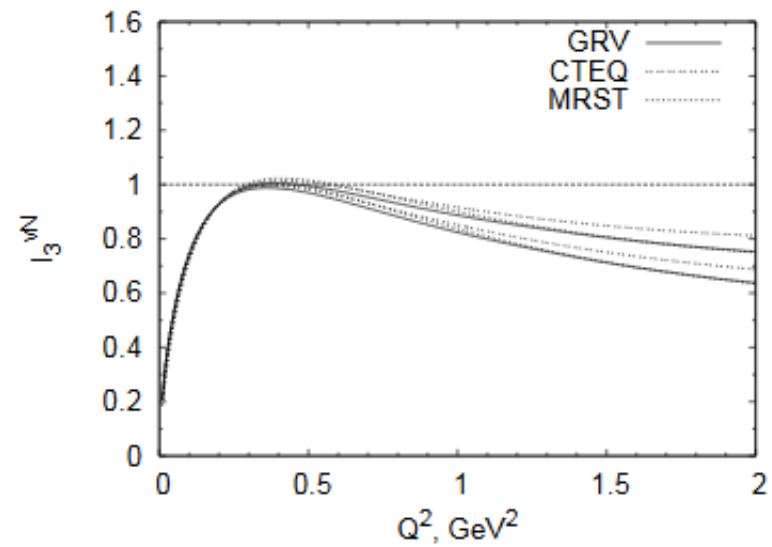
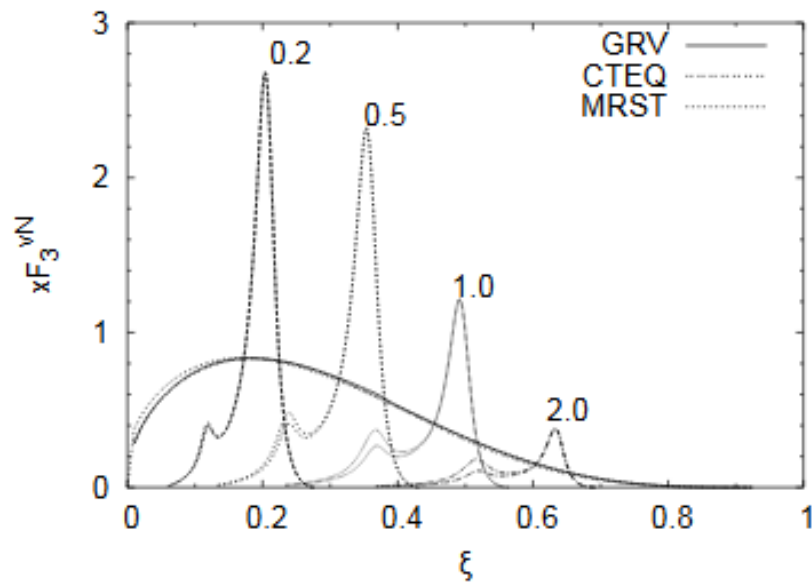
Dortmund model :  $P_{33}, D_{13}, P_{11}$  and  $S_{11}(1535)$  (Phys. Rev. C75,015201(2007)). Giessen model:13 resonances with GiBUU (AIP Conf.Proc. 1189 (2009) 276-282)





# Duality comparison for $xF_3(x)$

Lalakulich et al. Phys. Rev. C75, 2007



Comparing the resonances excited on an isoscalar target (deuterium) to the scaling curve in yellow.  
Niculescu et al. PRL 85(2000) 1182

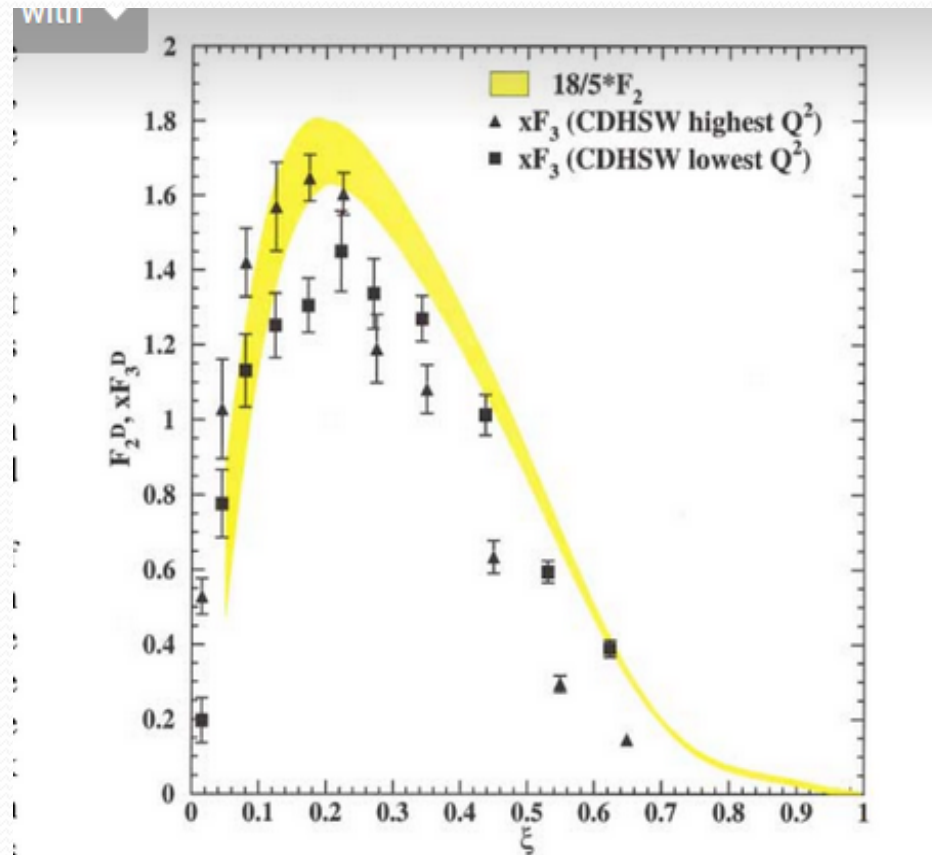


FIG. 3 (color). A comparison of the duality-averaged  $F_2$  scaling curve determined from the nucleon resonance region data from a deuterium target to the CDHSW data (Ref. [19]) on  $xF_3$  from deep inelastic neutrino-nucleus scattering data.

# Conclusions

- Understanding DIS as the scattering on quarks duality provides a picture on how the scaling limit is reached in the region  $x \rightarrow 1.0$ . The resonances slide down the shoulder present at  $0.8 < x < 1.0$ .
- At soft scattering resonances are formed, but when the interactions become more violent at larger values of  $Q^2$ , the resonances disappear, sliding down the scaling curve.
- Duality works better when diffraction is absent or subtracted. This is evident in the previous slide where  $x F_3(x)$  is compared to the scaling curve. The average over the resonances is correlated to the valence contribution.

# Duality in Nuclei

- Nuclei are made of protons and neutrons which are the partons (constituents) of nuclei. The resonances on nuclear targets will be their excited states, but for moderate values of  $Q^2$  and  $\nu$  the nuclei break up. The scaling limit for nuclei is a return to scattering on bound protons and neutrons. For this reason each channel, like quasi-elastic scattering or the production of the  $\Delta$ -resonance, is analyzed with a nuclear model in order to extract the cross sections for bound “protons” and “neutrons” including nuclear corrections.



# Carbon target

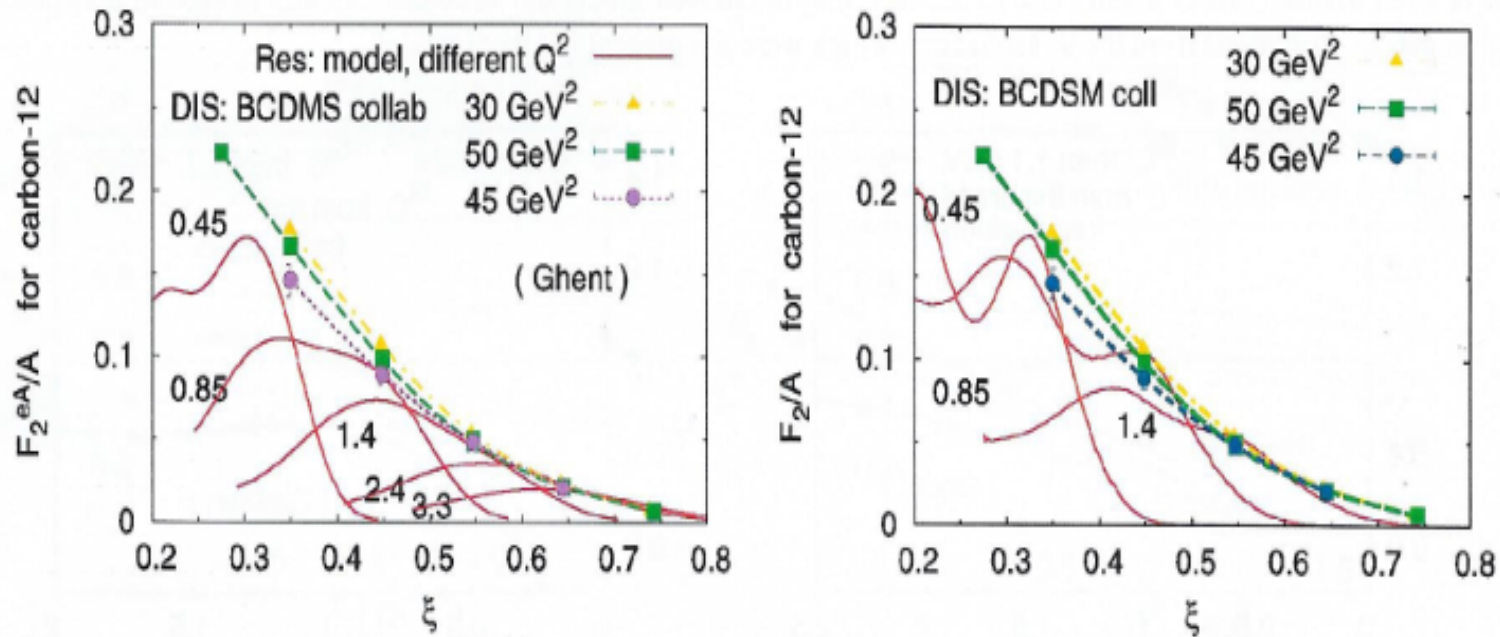



**FIGURE 3.** (Color online) Resonance curves  $F_2^{e^{12}C}/12$  as a function of  $\xi$ , for  $Q^2 = 0.45, 0.85, 1.4, 2.4$  and  $3.3$  GeV<sup>2</sup> (indicated on the spectra), obtained within Ghent (left) and Giessen (right) models, compared with the experimental data [23, 24] in the DIS region at  $Q_{DIS}^2 = 30, 45$  and  $50$  GeV<sup>2</sup>.



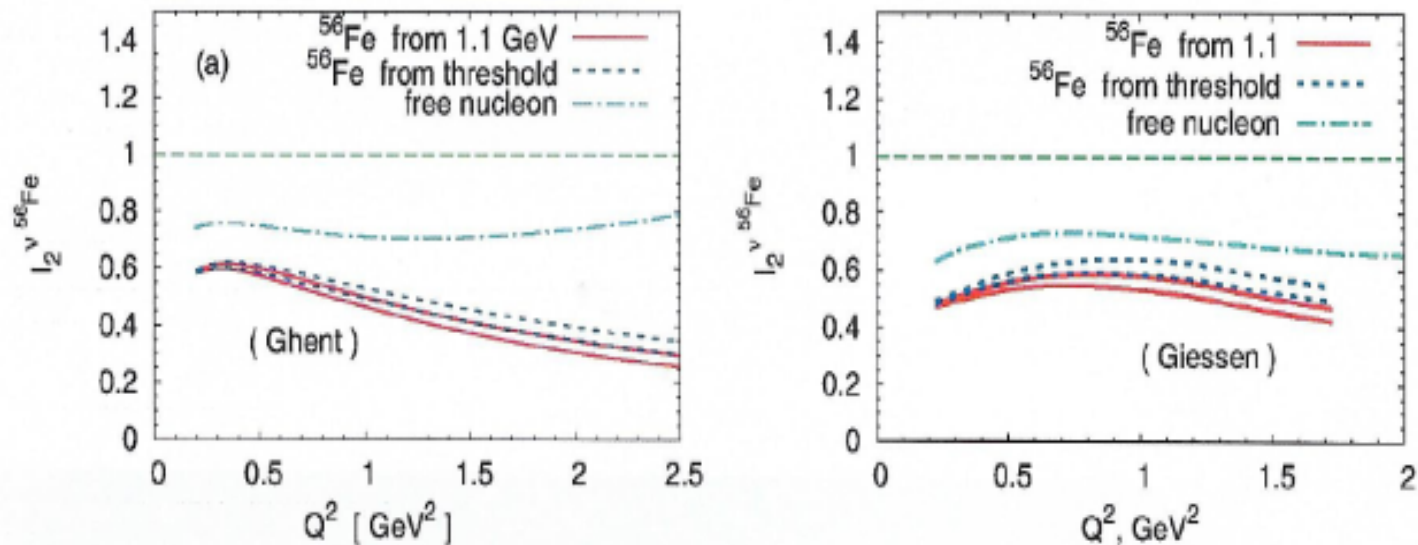


**FIGURE 6.** (color online) Ratio  $I_2^{\nu 56Fe}$  defined in Eq. (3) for the free nucleon (dash-dotted line) and  $^{56}Fe$  calculated within Ghent(left) and Giessen(right) models. For  $^{56}Fe$  the results are displayed for two choices of the underlimit in the integral:  $\bar{W} = 1.1$  GeV (solid line) and threshold (dotted line). For each of these two choices we have used two sets of DIS data in determining the denominator of Eq. (3). These sets of DIS data are obtained at  $Q_{DIS}^2 = 12.59$  and  $19.95$  GeV $^2$ .

- 
- The scaling curve per isoscalar nucleon is practically the same for free and bound nucleons.
  - Differences come for resonances , especially from the nuclear model of FSI and/or Fermi motion.
  - We must include bound state effects in order to extract the resonances.

Thus testing Duality on Nuclei is essentially a check of the model for nuclear corrections. We discuss several nuclear effects.

The Fermi motion modifies the energy and momentum distributions making the resonances wider. However, the integrated cross sections over the smeared width of the resonance remains the same [this is shown in the next slide where the width is folded with a Gaussian Fermi motion  $G(E',E)$  ].

# Smearing a resonance with a Gaussian

Assume a Gaussian distribution of energies around  $E$

$$G(E', E) = \frac{1}{\Delta E \sqrt{\pi}} e^{-\frac{(E'-E)^2}{(\Delta E)^2}} \quad \text{with} \quad \int_{-\infty}^{+\infty} G(E', E) dE' = 1$$

then

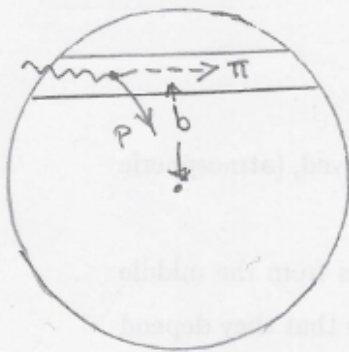
$$A(E) = \frac{1}{\Delta E \sqrt{\pi}} \int \frac{dE'}{(E' - M_R)^2 + \frac{\Gamma^2}{4}} e^{-\frac{(E'-E)^2}{(\Delta E)^2}} = \frac{2\sqrt{\pi}}{(\Delta E)\Gamma} e^{-\frac{(E-M_R)^2}{(\Delta E)^2}}$$

$$\int_{-\infty}^{+\infty} A(E) dE = \frac{2\pi}{\Gamma} = \int_{-\infty}^{+\infty} dE \frac{1}{(E - M_R)^2 + \frac{\Gamma^2}{4}}$$



In the ANP model of nuclear corrections, the resonances are affected by Fermi motion and absorption. Both corrections diminish quickly with increasing  $Q^2$ .

$$f(\lambda, L(b)) = \frac{1 - e^{-\kappa L(b)(1-\lambda P_+)}}{\kappa L(b)(1-\lambda P_+)}$$



1. Medium extends from  $x=0$  to  $b(b)$


2.  $\kappa = \rho(b)\sigma_{tot}$  is the inverse interaction length

3.  $P_+(\omega) = \frac{1}{3} \frac{\sigma_{\pi+p}(\omega) h_{\pm}(\omega)}{\sigma_{tot}}$   $h_{\pm} =$  Pauli blocking

$$4. f(\lambda) = \frac{\int_0^R b db L(b) f(\lambda, L(b))}{\int_0^{\infty} b db L(b)}$$

with  $L(b) = R\sqrt{\pi} e^{-b^2/R^2} \left\{ 1 + c \frac{1}{2} + \frac{b^2}{R^2} + c_1(\dots) \right\}$





In the ANP model a resonance is created at a point inside the nucleus with the cross section  $d\sigma(\pi k)$ . There are important nuclear effects, like the Fermi motion that I discussed. In addition there are: Pauli blocking and rescatterings described by a transport function  $f(1)$  that includes absorption. In the next slide I give typical values that show the magnitude of the effects.

The Pauli factor approaches 1.0 as  $Q^2$  increases .

$Q^2$	$g(Q^2, W)$
0.05	0.87
0.20	0.98
0.40	1.00

The transport function for various Nuclei:

Nucleus	$f(1)$
C(12)	0.81
N(14)	0.79
O(16)	0.81
Al(27)	0.72

# Carbon target

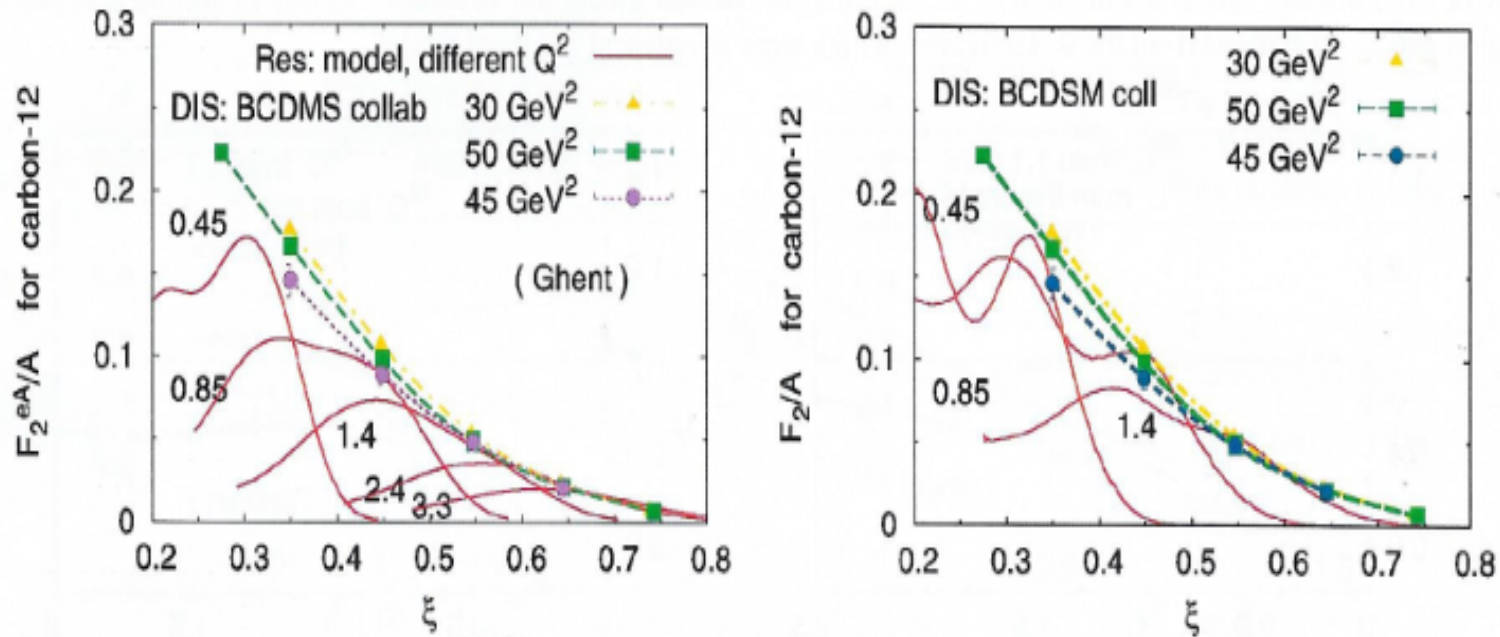


**FIGURE 3.** (Color online) Resonance curves  $F_2^{e^{12}C}/12$  as a function of  $\xi$ , for  $Q^2 = 0.45, 0.85, 1.4, 2.4$  and  $3.3 \text{ GeV}^2$  (indicated on the spectra), obtained within Ghent (left) and Giessen (right) models, compared with the experimental data [23, 24] in the DIS region at  $Q_{DIS}^2 = 30, 45$  and  $50 \text{ GeV}^2$ .

# Iron target

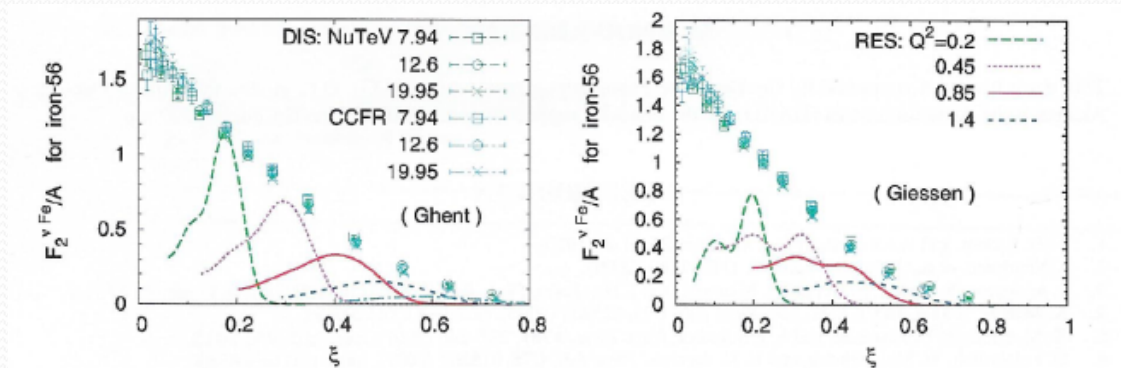


**FIGURE 5.** (color online) The computed resonance curves  $F_2^{v56Fe}/56$  as a function of  $\xi$ , calculated within Ghent(left) and Giessen (right) models for  $Q^2 = 0.2, 0.45, 0.85, 1.4$ , and  $2.4$  GeV<sup>2</sup>. The calculations are compared with the DIS data from Refs. [26, 27]. The DIS data refer to measurements at  $Q_{DIS}^2 = 7.94, 12.6$  and  $19.95$  GeV<sup>2</sup>.

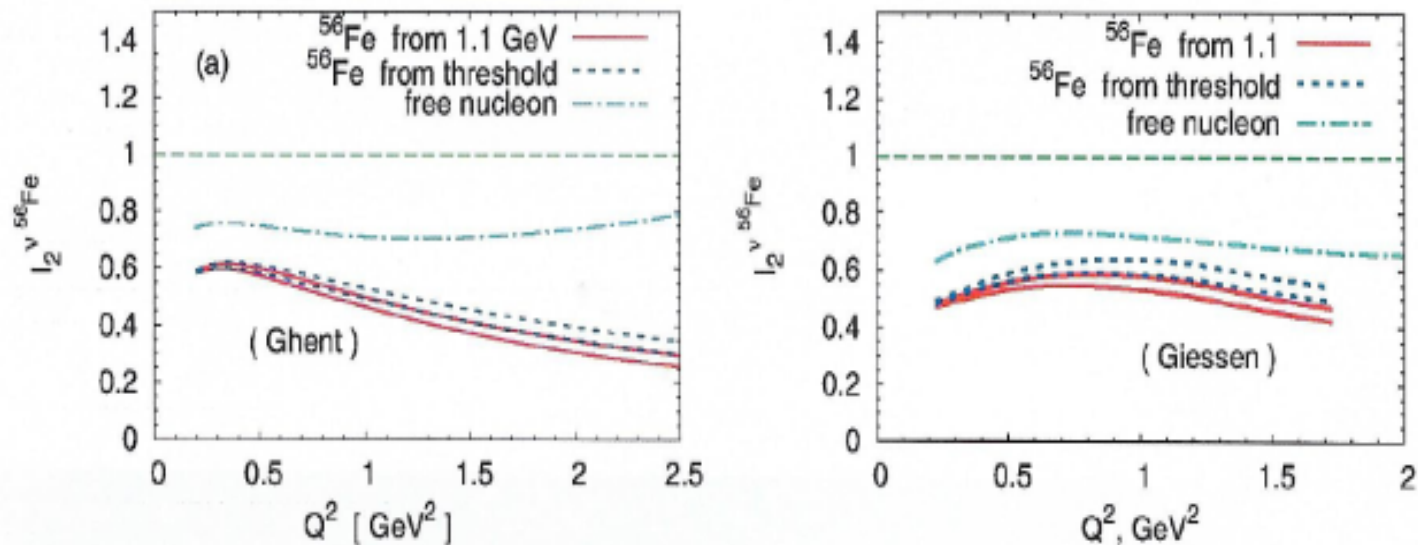



**FIGURE 6.** (color online) Ratio  $I_2^{\nu 56Fe}$  defined in Eq. (3) for the free nucleon (dash-dotted line) and  $^{56}Fe$  calculated within Ghent(left) and Giessen(right) models. For  $^{56}Fe$  the results are displayed for two choices of the underlimit in the integral:  $\bar{W} = 1.1$  GeV (solid line) and threshold (dotted line). For each of these two choices we have used two sets of DIS data in determining the denominator of Eq. (3). These sets of DIS data are obtained at  $Q_{DIS}^2 = 12.59$  and  $19.95$  GeV $^2$ .





# Summary

- An average over resonances is intimately related to the large  $x$  region of the scaling curve.
- Resonances without diffractive scattering are correlated to the valence component of the scaling curve.
- We have a dual picture for the interactions of the proton with currents: one with resonances and another with scaling. We found a kinematic relation between them. However, there is not yet an analytic method describing how one description merges into the other.

- 
- We hope to obtain information how the scattering on confined quarks develops into bound states. For instance, duality dictates relations among channels of electro- and neutrino-production of the Delta and other resonances in order to satisfy the relation

$$F_2(eN) = 5/18 F_2(\nu N) .$$

- For nuclei we must still understand how to extract from data the resonances produced by neutrinos on bound “proton” and “neutron”, then compare the results with the structure functions. New models on this topic are desirable.

